forests

MDPI

Article

Impacts of Climate Change on Wildfires in Central Asia

Xuezheng Zong [1], Xiaorui Tian [1,*] and Yunhe Yin [2]

[1] Research Institute of Forest Ecology, Environment and Protection, Chinese Academy of Forestry, Key Laboratory of Forest Protection of National Forestry and Grassland Administration, Beijing 100091, China; zongxuezheng1995@163.com

[2] Key Laboratory of Land Surface Pattern and Simulation, Institute of Geographic Sciences and Natural Resources Research, Chinese Academy of Sciences, Beijing 100101, China; yinyh@igsnrr.ac.cn

* Correspondence: tianxr@caf.ac.cn; Tel.: +86-10-6288-9849

Received: 18 June 2020; Accepted: 24 July 2020; Published: 25 July 2020

Abstract: This study analyzed fire weather and fire regimes in Central Asia from 2001–2015 and projected the impacts of climate change on fire weather in the 2030s (2021–2050) and 2080s (2071–2099), which would be helpful for improving wildfire management and adapting to future climate change in the region. The study area included five countries: Kazakhstan, Kyrgyzstan, Tajikistan, Uzbekistan, and Turkmenistan. The study area could be divided into four subregions based on vegetation type: shrub (R1), grassland (R2), mountain forest (R3), and rare vegetation area (R4). We used the modified Nesterov index (MNI) to indicate the fire weather of the region. The fire season for each vegetation zone was determined with the daily MNI and burned areas. We used the HadGEM2-ES global climate model with four scenarios (RCP2.6, RCP4.5, RCP6.0, and RCP8.5) to project the future weather and fire weather of Central Asia. The results showed that the fire season for shrub areas (R1) was from 1 April to 30 November, for grassland (R2) was from 1 March to 30 November, and for mountain forest (R3) was from 1 April to 30 October. The daily burned areas of R1 and R2 mainly occurred in the period from June–August, while that of R3 mainly occurred in the April–June and August–October periods. Compared with the baseline (1971–2000), the mean daily maximum temperature and precipitation, in the fire seasons of study area, will increase by 14%–23% and 7%–15% in the 2030s, and 21%–37% and 11%–21% in the 2080s, respectively. The mean MNI will increase by 33%–68% in the 2030s and 63%–146% in the 2080s. The potential burned areas of will increase by 2%–8% in the 2030s and 3%–13% in the 2080s. Wildfire management needs to improve to adapt to increasing fire danger in the future.

Keywords: climate change; fire weather; MNI; fire season

1. Introduction

Wildfires are a dominant disturbance in most forests and are strongly influenced by climate [1]. Climate warming has recently caused changes in the fire regime in the Northern Hemisphere [2], which has experienced extreme wildfire seasons and fire frequency increases in forests. Notably, high-intensity fires have occurred in summer in some regions. During the summer of 2010, climate warming caused several hundred wildfires and burned areas of approximately 5 million ha in Russia [3]. In the summer of 2017, British Columbia, Canada, experienced the worst wildfire, which caused a burned area of 1.2 million ha [4]. In addition, in the boreal forest of North America, climate warming has led to greater and more severe wildfire activity, increased fire frequency and fire sizes, and longer fire seasons [5]. The large-scale wildfires in the United States in 2019 and Australia from 2019–2020 attracted the attention of global society. Central Asia is located in the arid and semiarid zone, which includes

Kazakhstan, Kyrgyzstan, Tajikistan, Uzbekistan, and Turkmenistan [6]. Wildfires caused great losses in forest resources and properties in the region. The region is an important region for global biodiversity and has important species, such as snow leopards and brown bears [7]. Currently, Central Asian countries are in a critical period of economic and social transformation and are important components of "the Belt and Road". The countries in the region have made great efforts to increase the forest coverage rate and enhance biodiversity [8]. It is important to protect the existing forest resources to improve the ecological environment in Central Asia, which would be helpful for improving the living environment of local residents and promoting economic development.

Climate change will increase fire danger, and potential wildfires will increase significantly around the world in the future [9,10]. Additionally, climate change has increased wildfires in northern Europe and Greenland [11–13]. The fifth assessment report of the IPCC indicated that future wildfire risk would increase and that the fire season would become longer in southern Europe [14]. Compared to the present scenario, the annual burned area was projected to increase three to five times under the A2 scenario by 2100 [14]. The frequency of fires will increase to 25% by 2030 and 75% by the end of the 21st century in Canada, under the Canadian Climate Centre GCM (general circulation models) scenarios, and fire occurrence will increase by 140% under the Hadley Centre GCM scenario [15]. The higher number of wildfires resulted in an increased budget for fire management. In Russia, increasing wildfire frequency is expected to cause the total cost of forest fire management to increase by 211,114 and 248,956 thousand rubles (approximately 286.6–340 million US$) by the end of the 21st century [16]. Therefore, the study of future fire weather under different climate scenarios for the region would be the basis for adapting to future climate change.

There are many wildfires each year in Central Asia, especially in Kazakhstan [17]. Wildfires frequently occurred and damaged forest resources in these countries due to less fire management. The annual average burned forest area was 4000 ha in Kazakhstan during the 1985–1990 period and increased to 20,000 ha during the 1996–2000 period. In 1997, the annual burned area was 200,000 ha [18]. However, there were just 486 forest fires and 3915 ha of burned areas in 2012 in Kazakhstan [19]. Grassland fires occur frequently in Central Asia [20]. The mean annual burned areas of grasslands in the broader steppe-dominated region was 15 million ha during the 2001–2009 period, which mainly occurred in August and September [21]. Potential wildfires in the future will increase due to climate warming and may cause more burned areas and environmental pollution [9,22]. There have been some studies on the fire risk of Kazakhstan [23,24], but little research has been conducted on the fire regime of Central Asia. Therefore, it would be interesting to study the fire weather and fire regime in Central Asia and further evaluate fire danger under future climate scenarios.

The Fire Weather Index can effectively describe the relationship between weather and fire danger [25]. Bedia et al. found that the FWI (Fire Weather Index) in the grasslands of Kazakhstan was higher than that in other regions during the 1981–2000 period [26]. However, they only analyzed fire danger on a global scale by using WFDEI data. The FWI calculation requires inputs of noon temperature, relative humidity, wind speed, and 24-h accumulated precipitation. It is difficult to obtain enough weather observation data covering the vegetation areas in Central Asia. Some fire weather indices developed in the former Soviet Union, such as the Nesterov index (NI) [27], Zhdanko index (ZhI) [28], and Modified Nesterov index (MNI) [29], are widely used in Russia and countries in Central Asia [30–33]. These indices are calculated with mid-day temperature, dew point deficit, and precipitation and need fewer inputs than the FWI.

The objective of this study was to analyze fire weather by using MNI and fire regimes for each vegetation zone in Central Asia. We will define the fire seasons for each vegetation zone based on the process of the daily fire weather index and burned area and evaluate the potential fire danger in the 2030s and 2080s under future climate scenarios.

2. Methods

2.1. Study Area

Central Asia is located in central Eurasia and is adjacent to China in the west and the Caspian Sea in the west. Its geographical range is 35°08′–55°25′ N, 46°28′–87°29′ E. The total area is approximately 3970 million ha. It has a temperate continental climate and uneven distribution of rainfall. The annual precipitation ranges from 100–400 mm, and it can be more than 500 mm in high mountain areas and less than 200 mm on plains [7].

The forest coverage rate in the study area was 1.6%, which was mainly distributed in the northeast. Shrubs were mainly distributed in the western and central parts of the study area, with a coverage rate of 22.4%. Grassland and farmland accounted for 23.8% and 20.3%, respectively (Figure 1).

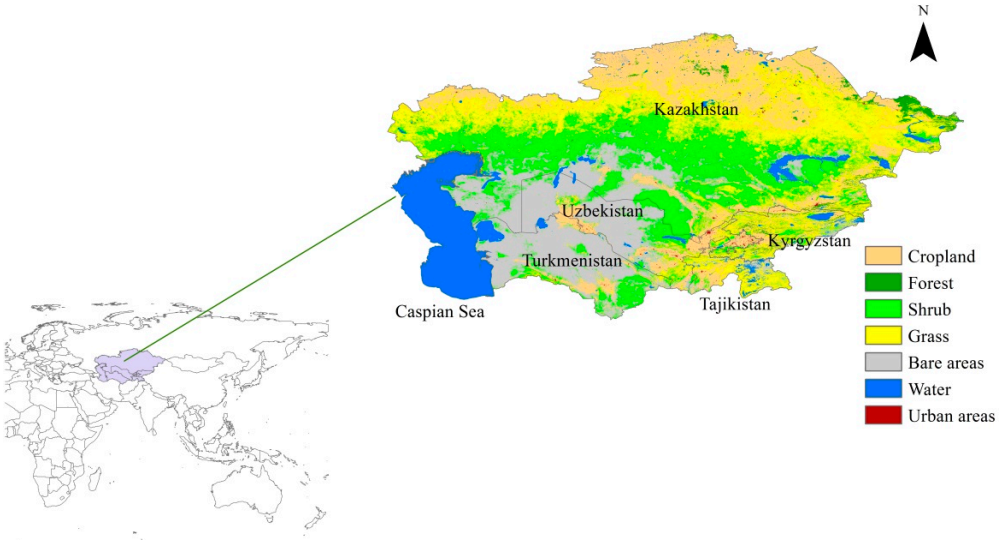

Figure 1. Location of the study area and vegetation types.

2.2. Data Sources

Land cover data (2001–2015, 300 m spatial resolution) were downloaded from the land cover state products of the European Space Agency (https://www.esa-landcover-cci.org, accessed on 17 January 2020), which include forest, grassland, shrub, and water. The historical daily meteorological data (2001–2015) came from the global historical meteorological network (https://data.nodc.noaa.gov), including eighteen weather stations located in the forest and grassland. The daily data included the maximum temperature, minimum temperature, 24 h precipitation, and dew point. MODIS-MCD64A1 products (2001–2015, 500 m spatial resolution and daily resolution in temporal) were obtained from NASA (https://earthdata.nasa.gov, accessed 17 January 2020).

The simulated climate data (1971–2099, 0.5° × 0.5° resolution) of the HadGEM2-ES global climate model with four climate scenarios (RCP2.6, RCP4.5, RCP6.0, and RCP8.5) (GCM) were downloaded from the Inter-Sectoral Impact Model Intercomparison Project (ISI-MIP) (https://www.isimip.org/, accessed 17 January 2020). The daily climate data included maximum temperature, minimum temperature, and precipitation.

2.3. Climate Data Processing

For the missing temperature and dew point temperature in historical observation data for the 2001–2015 period, we used the sliding average of the before and after five days to replace the missing data. Due to the lack of daily precipitation data, data from neighboring meteorological stations were used.

The precipitation frequency from the historical climate data was used to correct the simulated precipitation frequency of the simulated climate data. We assumed that the daily precipitation frequencies of the simulated data were identical to the historical data (2001–2015). We obtained the precipitation threshold based on its frequency and set the data less than the threshold to zero. Then, we used the coefficient between the simulated annual precipitation and reserved data to correct the daily precipitation.

The mid-day temperature was replaced with the maximum temperature minus the average difference (2 °C). The dew point temperature was calculated from the daily minimum temperature. The calculation formula was developed with the dew point temperature above 0 °C and the daily minimum temperature in each month of the historical observation data.

2.4. Fire Weather Indices Calculation

The modified Nesterov index was calculated with the following equation [29]:

$$MNI(n) = (MNI(n-1) + T \times d) \times K(n) \quad (1)$$

where $MNI(n-1)$ and $MNI(n)$ are the fire weather index on days $n-1$ and n, respectively. T is the mid-day temperature, d is the dew point temperature, $K(n)$ is a scale coefficient that controls the index change when precipitation occurs on day n [33] (Table 1).

Table 1. The corresponding relationship between coefficient *K* and daily precipitation.

Rain/mm	0	0.1–0.9	1.0–2.9	3.0–5.9	6.0–14.9	15.0–19.9	≥20.0
K	1.0	0.8	0.6	0.4	0.2	0.1	0

2.5. Vegetation Zone

The study area can be divided into four zones based on the vegetation types, which include shrub (R1), grassland (R2), mountain forest (R3), and rare vegetation zone (R4) (Figure 2). This paper focuses on zones with vegetation, such as R1, R2, and R3.

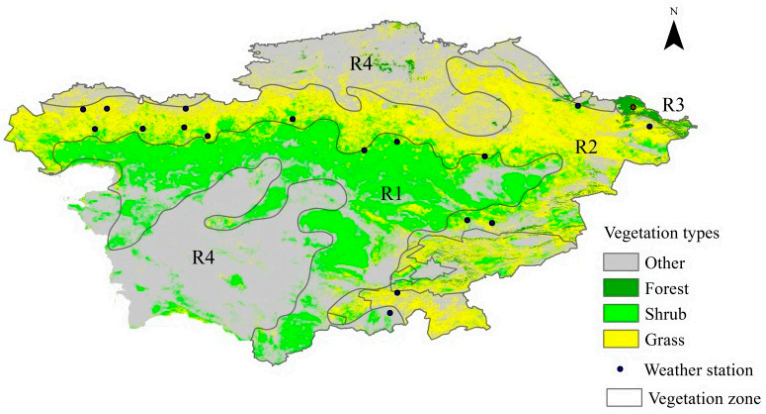

Figure 2. Vegetation zones and weather stations in the study area.

2.6. Burned Areas

The fire season and land cover data were used to filter the false burned areas of the MODIS-MCD64A1 products. Then, we obtained the daily burned areas of each vegetation zone.

2.7. Data Processing

SPSS software was used to analyze the correlation between the fire weather index and burned area. The MNI of each zone was interpolated with the kriging method.

3. Results

3.1. Fire seasons for Each Vegetation Zone

The daily MNI of each vegetation zone was roughly normally distributed. The MNI increased slowly for 90 days and decreased rapidly from the peak. The MNI of R1 increased from the 95th day (Julian day), reached a maximum on the 280th day, and remained at a very low level after the 325th day (Figure 3(a1)). In R2, the MNI increased from the 95th day (peak on the 283rd day) and was maintained at a very low value after the 342nd day. In R3, the MNI increased from the 125th day and decreased to a very low value after the 300th day (maximum on the 248th day).

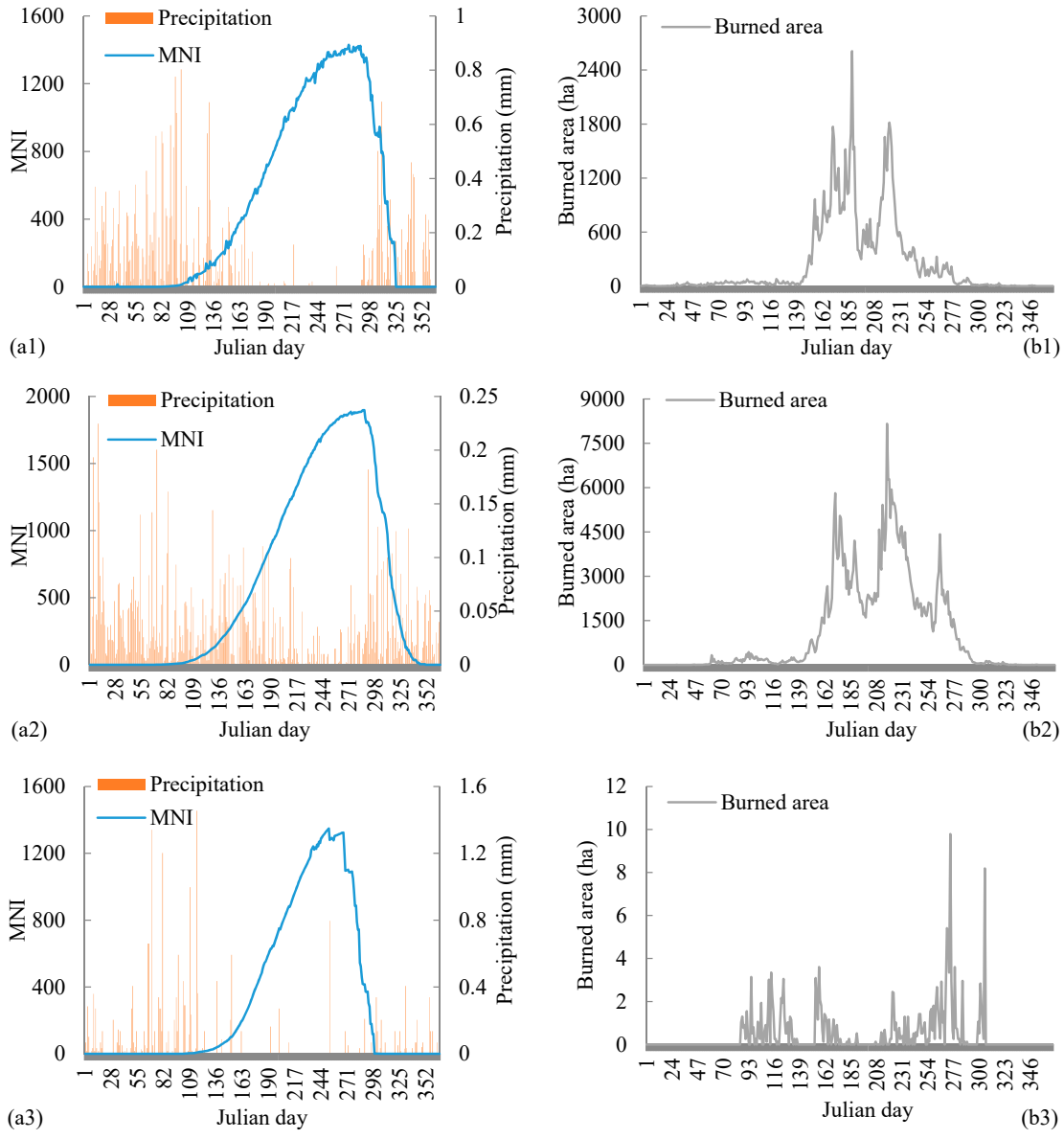

Figure 3. Mean daily modified Nesterov index (MNI), precipitation, and burned areas for the three vegetation zones from 2001–2015. (**a1**) the mean daily MNI and precipitation for vegetation zones R1; (**a2**) the mean daily MNI and precipitation for vegetation zones R2; (**a3**) the mean daily MNI and precipitation for vegetation zones R3; (**b1**) the mean daily burned areas in R1; (**b2**) the mean daily burned areas in R2; (**b3**) the mean daily burned areas in R3.

The fire season of each vegetation zone could be defined by the fire weather index and the daily burned areas. The daily burned areas for R1, R2, and R3 showed apparent changes during the periods of days 150–280, 140–300, and 90–305, respectively (Figure 3(b1–b3)). However, there were some grass fires during days 60–140. The dates of the increases in daily burned areas were earlier than that of the increases in MNI. In early spring, the fuels are dry and cured grass, which can burn at low MNI conditions. The date when the daily burned areas decreased to zero was also earlier than the date when the MNI reached a very low value. The MNI only indicates fire weather, which does not reflect the seasonal status of live fuel. Although daily burned areas showed a relationship with the MNI ($r > 0.23$), their changes were not completely consistent.

The fire season of each zone was defined based on the process of daily MNI and burned areas, which were 1 April–30 November for R1, 1 March–30 November for R2, and 1 April–31 October for R3.

During the period from 2001–2015, the mean MNI in the R1 fire season was 10,213. The high MNI values were distributed in the central areas, especially in the middle part near R2 (MNI > 12,000) (Figure 4). The mean MNI of R2 was 12,104, and the high MNI values were distributed in the northwestern and south-central parts. The mean MNI of R3 was 10,769 (Figure 4).

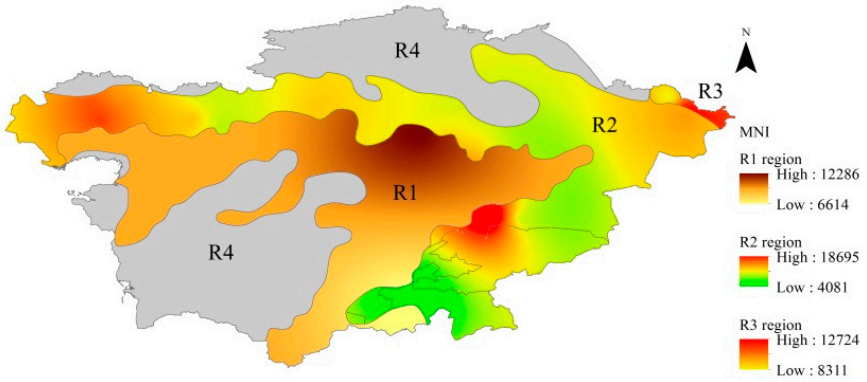

Figure 4. MNI distribution in three vegetation zones for the 2001–2015 period.

3.2. Distribution of Burned Areas in the 2001–2015 Period

The mean annual burned area was 87,812 ha in R1 during the 2001–2015 period. The burned areas in 2002, 2004, and 2005 were significantly higher than the average of the period ($\alpha = 0.05$), and the burned areas were significantly lower in 2001, 2003, 2011, 2012, and 2013 (Figure 5(a1)). The monthly maximum burned areas occurred in May, with 26,603 ha, and the minimum occurred in November, with 250 ha (Figure 5(b1)). The mean annual burned area in R2 was 389,020 ha, which was much higher than that in the other zones. The maximum monthly burned area was 133,452 ha in August, and the minimum was 1211 ha in November. The mean annual burned area in R3 was 150 ha. The months in the fire season with the maximum and minimum burned areas were September and June, respectively (Figure 5(b3)).

The monthly burned areas and MNI in the fire season for R1 and R3 did not show a strong correlation ($r = 0.36$), but they showed a strong correlation for R2 ($r = 0.6$) as follows:

$$B(n) = 2.4683MNI(n) + 13,101 \ (R^2 = 0.32) \quad (2)$$

where, $B(n)$ and $MNI(n)$ are the burned areas and mean MNI in month n.

Grass fires and shrub fires mainly occurred in the period from June to September, and they were usually distributed in the plains and hilly areas with elevations less than 500 m. There were no wildfires in the areas with elevations greater than 2000 m. The fires in mountain forests mainly occurred in the April–June and September–October periods and were usually distributed the areas with low elevation

(<500 m). A few wildfires also occurred in high-altitude areas (>1500 m ASL) during July and August (Figure 6).

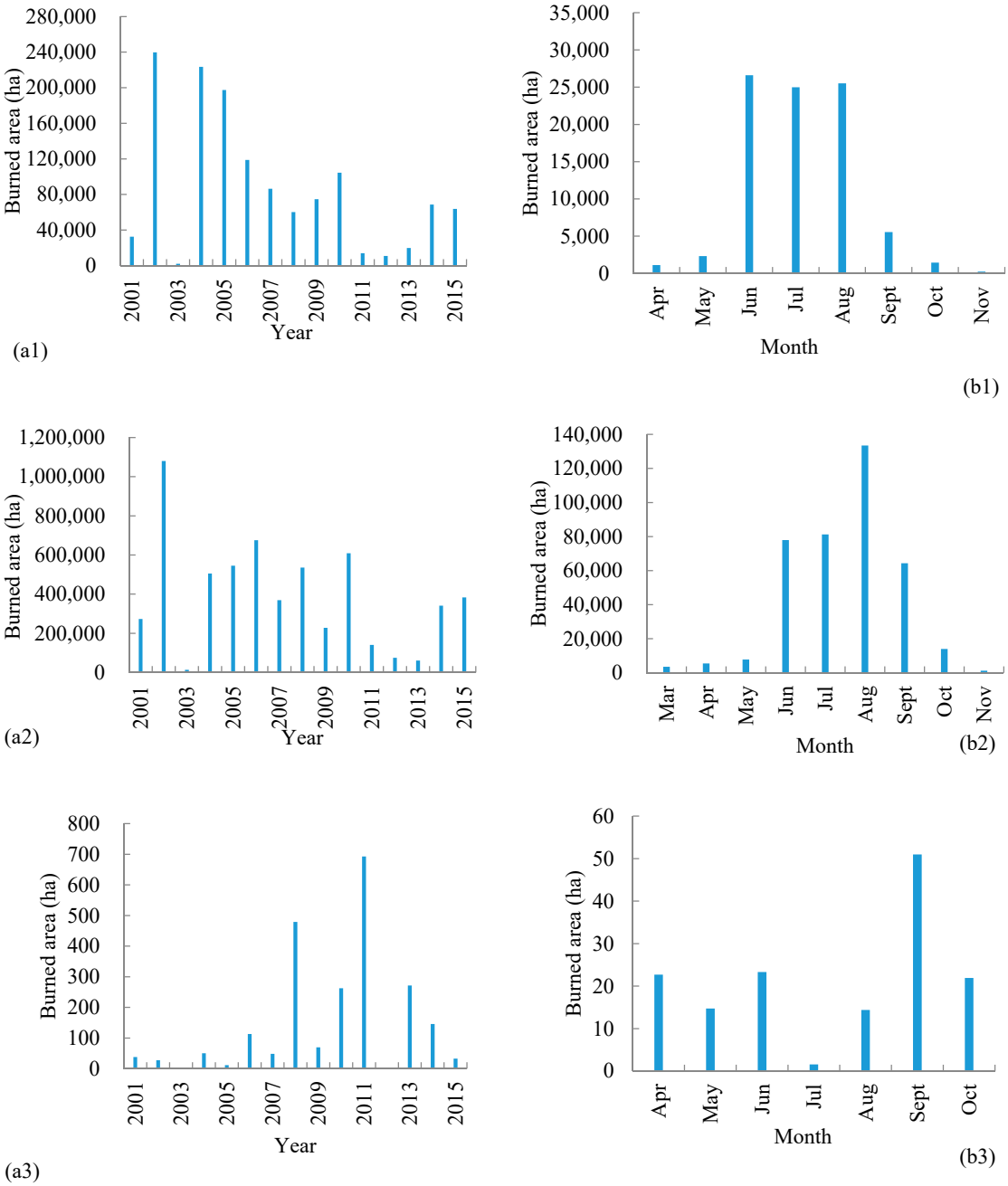

Figure 5. Annual and monthly burned areas for three vegetation zones during the 2001–2015 period. (**a1**) the mean annual burned areas in R1; (**a2**) the mean annual burned areas in R2; (**a3**) the mean annual burned areas in R3; (**b1**) the mean monthly burned areas in R1; (**b2**) the mean monthly burned areas in R2; (**b3**) the mean monthly burned areas in R3.

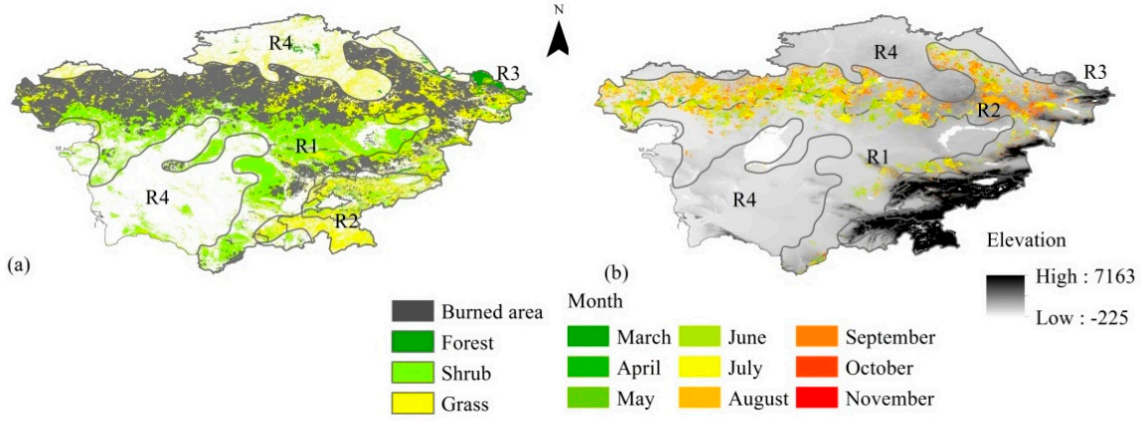

Figure 6. Burned area distribution in the study area during the 2001–2015 period.

3.3. Climate Change in the 2030s and 2080s

The mean daily maximum temperature in the fire season of R1 was 23.2 °C during the baseline period. It will be 26.4 °C band 28.2 °C in the 2030s and 2080s, respectively, which will be an increase of 14% and 21% compared with the baseline (p = 0.00). The precipitation in the fire season of R1 was 180 mm at the baseline and will be 219, 174, 198, and 180 mm under the RCP2.6, RCP4.5, RCP6.0, and RCP8.5 scenarios in the 2030s, respectively. The precipitation will increase by 7% to 193 mm in the 2030s. However, the increase was not significant (F-test, p = 0.12). In the 2080s, the precipitation will be 215, 195, 178, and 214 mm under the RCP2.6, RCP4.5, RCP6.0, and RCP8.5 scenarios, respectively. The mean precipitation will significantly increase by 11% to 200 mm in the 2080s (F-test, p = 0.04) (Figure 7).

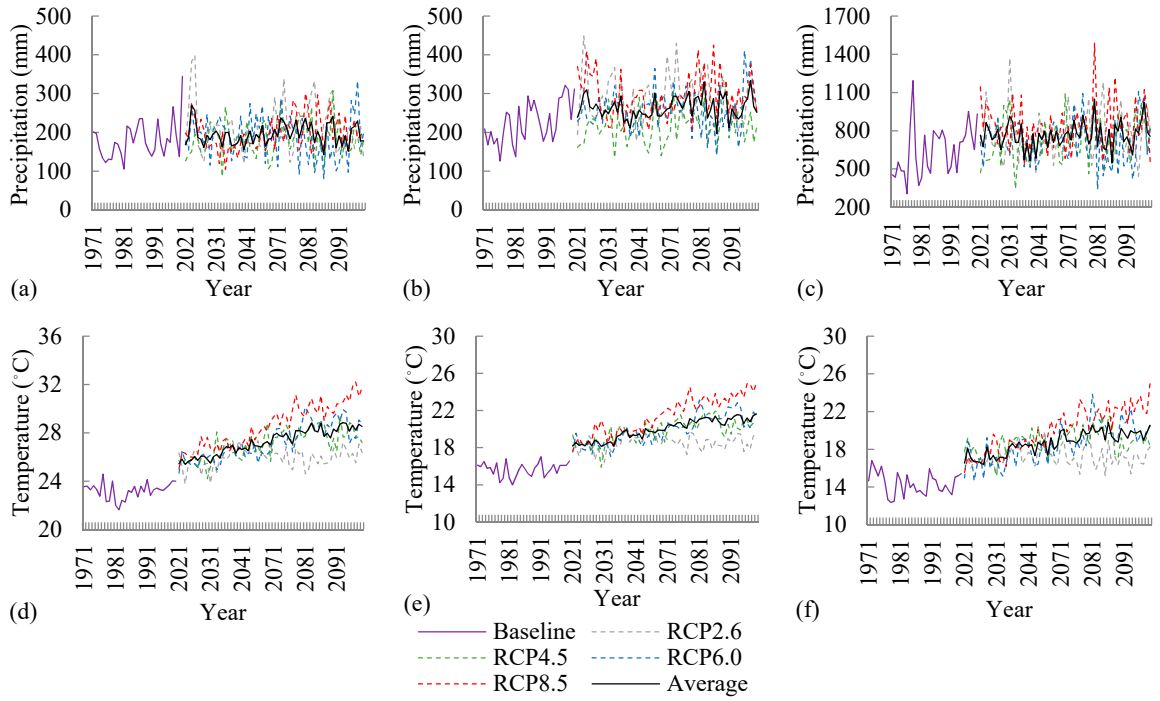

Figure 7. Precipitation and temperature in the fire season for three vegetation zones in the baseline, 2030s, and 2080s. (**a**) the precipitation during the fire season in the R1; (**b**) the precipitation during the fire season in the R2; (**c**) the precipitation during the fire season in the R3; (**d**) the mean daily maximum temperatures of the fire season in the R1; (**e**) the mean daily maximum temperatures of the fire season in the R2; (**f**) the mean daily maximum temperatures of the fire season in the R3.

The mean daily maximum temperature in fire season of R2 was 15.7 °C in the baseline period. It will significantly increase by 21% and 34% in 2030s and 2080s, respectively ($p = 0.00$). The precipitation in fire season of R2 was 226 mm at the baseline, and it will be 293, 206, 256, and 284 mm in the 2030s under the RCP2.6, RCP4.5, RCP6.0, and RCP8.5 scenarios, respectively. The mean precipitation will increase 15% in 2030s ($p = 0.00$). In addition, the precipitation in the fire season will significantly increase by 21% in 2080s ($p = 0.00$), and the precipitation will be 294, 231, 260, and 303 mm under the RCP2.6, RCP4.5, RCP6.0, and RCP8.5 scenarios, respectively.

In R3, the mean daily maximum temperature in fire season was 14.3 °C in baseline. It will increase by 23% to 17.7 °C in 2030s, when the temperature will be 17.3, 18.2, 17.2, and 18.2 °C under the RCP2.6, RCP4.5, RCP6.0, and RCP8.5 scenarios, respectively. In 2080s, the mean daily maximum temperature will significantly increase to 19.6 °C ($p = 0.00$), which will be 17.2, 19.4, 20.0, and 21.9 °C under the RCP2.6, RCP4.5, RCP6.0, and RCP8.5 scenarios, respectively. The precipitation in fire season was 646 mm at the baseline and will be 743, 696, 718, and 817 mm under RCP2.6, RCP4.5, RCP6.0, and RCP8.5 scenarios in the 2030s, respectively. In 2080s, the mean precipitation will increase significantly to 784 mm ($p = 0.00$), representing an increase of 21% from the baseline.

3.4. MNI Changes in the 2030s and 2080s

The mean MNI in the fire season of R1 was 3812 at the baseline, and it will increase by 33% and 63% in the 2030s and 2080s, respectively ($p = 0.00$) (Figure 8). In R2, the mean MNI of the fire season was 1759 at baseline, and it will increase by 42% in the 2030s and 73% in the 2080s ($p = 0.00$). The mean MNI of the fire season for R3 was 713 at baseline, and it will increase to 1195 in the 2030s and 1752 in the 2080s ($p = 0.00$).

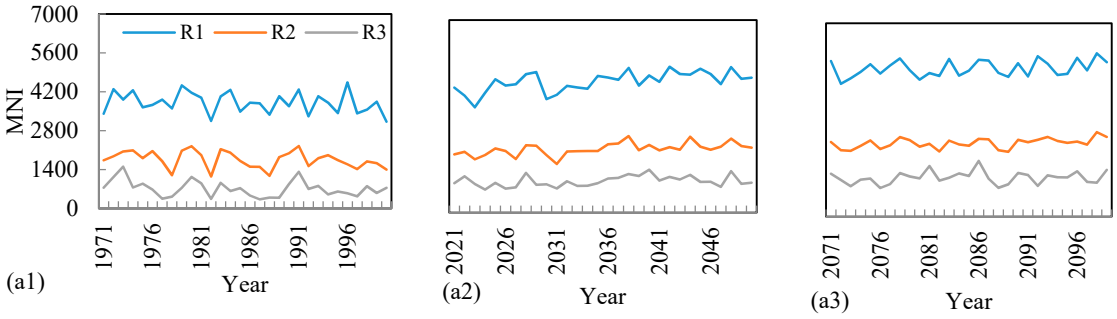

Figure 8. Mean MNI of fire season for three vegetation zones in different period. (**a1**) mean MNI of fire season in baseline; (**a2**) mean MNI of fire season in 2030s; (**a3**) mean MNI of fire season in 2080s.

Most areas of R1 showed low MNI values (<4691) at the baseline, and only southern areas had high MNI values (8735–17,156) (Figure 9(a1)). In the 2030s, the MNI values in western and northern R1 showed a slight increase but will increase from 23%–30% in central areas and 37%–59% in the south. The mean MNI will increase by 19%, 28%, 20%, and 33% in the 2030s under the RCP2.6, RCP4.5, RCP6.0, and RCP8.5 scenarios, respectively. The MNI will increase obviously under scenarios RCP4.5 and RCP8.5, and the maximum increase will reach 68% and 82%, respectively (Figure 9(b3,b5)). In the 2080s, MNIs will increase by more than 37% in central and southern R1, while MNIs in western R1 will increase by only 15% (Figure 9(c1)). The mean MNI will increase by 15%, 39%, 46%, and 64% over the baseline under the RCP2.6, RCP4.5, RCP6.0, and RCP8.5 scenarios, respectively. Under the RCP2.6 scenario, the MNI will increase significantly in the south, while the MNI will increase in the central and southern regions significantly under the other scenarios.

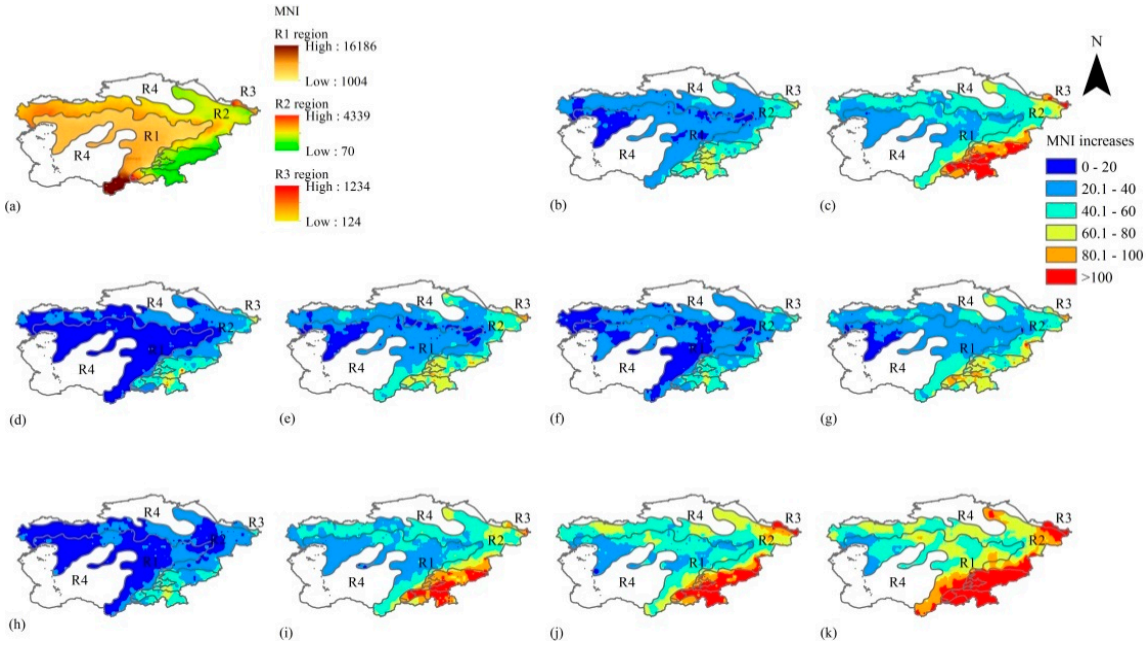

Figure 9. Distribution of MNI in the fire season for each vegetation zone. (**a**) Baseline; (**b**) the mean MNI increase in the 2030s; (**d**), (**e**), (**f**), and (**g**) are MNI increases under the RCP2.6, RCP4.5, RCP6.0, and RCP8.5 scenarios in the 2030s, respectively; (**c1**) the mean MNI increase in the 2080s; and (**h**), (**i**), (**j**), and (**k**) are MNI increases under the RCP2.6, RCP4.5, RCP6.0, and RCP8.5 scenarios in the 2080s, respectively.

The MNI values in western R2 were high at baseline. The mean MNI will increase by 23%, 35%, 26%, and 42% in the 2030s under the RCP2.6, RCP4.5, RCP6.0, and RCP8.5 scenarios, respectively. The increase is significant for the RCP4.5 and RCP8.5 scenarios. The MNI in the southern area will increase clearly (+50%), but the values in the western areas will increase by only 10%–38% in the 2030s. The MNI will increase by 20%, 51%, 61%, and 73% in the 2080s under the RCP2.6, RCP4.5, RCP6.0, and RCP8.5 scenarios, respectively. The MNI values in the western and southern R2 will increase significantly under RCP2.6 scenario, and the values will increase significantly in the western, central, and southern areas under the other scenarios.

The MNI values were high in the northwest of R3 (1163–1353) and low in the southeast (322–599) at the baseline. The mean MNI will increase by 49%, 77%, 49%, and 68% in the 2030s over the baseline under the RCP2.6, RCP4.5, RCP6.0, and RCP8.5 scenarios, respectively. In the 2080s, the mean MNI will increase by 32%, 84%, 127%, and 146% under the RCP2.6, RCP4.5, RCP6.0, and RCP8.5 scenarios, respectively. A greater increase in MNI will be distributed in the northwestern and central areas under the RCP2.6 scenario, while MNI will increase clearly in the northwest of R3 under the other scenarios.

4. Discussion

The MNI can effectively reflect drought weather and fuel moisture in Central Asia [33]. In the study area, there was less precipitation and higher temperatures from June–September, and the MNI reached its peak in August or September. Burned area is the most important indicator of fire regime. We used the daily burned areas from 2001–2015 from MODIS data to describe their distributions spatially and temporally [34]. There have been some studies on wildfires in Central Asia based on remote sensing data in recent years [21,35,36]. We determined the fire season for each vegetation zone according to the MNI and daily burned areas. We considered the characteristics of fire regime and fire weather. The defined fire season would be an important indicator of fire dynamics and fire management in the region.

Grassland fire and shrub fire mainly occurred in summer (June–September), and the largest burned areas in grassland usually occurred in August or September [21]. The fires in mountain forests in the low altitude regions mainly occurred in spring (April–June) and autumn (September and October). Nevertheless, the fires mainly occurred in summer (July and August) for the forests at high-altitude areas (>1500 m ALS). Fires in mountain forests are usually distributed in areas near farmland or towns, which indicates that human activities impact these occurrences. The references indicated that most forest fires were ignited by humans in low-altitude areas and fires in high-altitude areas in summer were mainly caused by lightening [4,18].

Although both the temperature and temperature in the fire season of the vegetation zones will increase in the 2080s under future climate scenarios, their MNIs will still increase clearly over the baseline. This indicates that fire danger will increase in the future, which is consistent with the results of Liu et al. [9]. They also believed that the mean daily maximum temperature and fire danger rating of Central Asia (HadCM3 model with A2a scenario) would increase from 2071–2100, but they projected that the annual precipitation would decrease.

Climate change will also affect the vegetation of the study area. In the study we did not simulate the vegetation change resulting from the future climate change. Vegetation distribution was affected by many factors, such as climate, anthropic activities, and natural disturbances. In fact, forest and grassland decreased during the period 1992–2003 and increased slightly during 2003–2015. However, vegetation types and their spatial distribution was no changed clearly in the period [37]. We assumed that the vegetation will not signification change in the coming decades. This point will not have influences on the judgment of fire weather changes under the future climate scenarios.

The fewer meteorological stations (18) available from 2001–2015, and their uneven spatial distribution, may affect the interpolated results of fire weather. However, each meteorological factor and fire weather index showed very similar processes in those years. The influence would not affect the reliability of the results.

Fire weather affects ignitions and fire spread. The MNI showed a positive correlation with the monthly burned areas ($r < 0.3$). Based on the correlation, we projected that the potential burned areas would increase in the future. The potential burned areas of R1, R2, and R3 in the 2030s will increase by 4%, 8%, and 2% over the baseline and will increase by 6%, 13%, and 3%, respectively, in the 2080s.

The wildfires were mainly distributed in shrub and grassland areas. The annual burned area has generally declined since 2010. This trend reflects the role of fire management activities. The governments in Central Asia established fire agencies and promulgated laws and regulations on wildfire management in this century [38]. The wildfires were still serious in some years (such as 2011). The vegetation in the study area plays an important role in the regional ecological environment and biodiversity protection [39]. It is necessary to strengthen wildfire management in the region to adapt to future climate change.

5. Conclusions

Fire seasons are different for each vegetation zone. Grassland has the longest fire season, and mountain forests have the shortest fire season. The fire seasons of grassland, shrub, and mountain forest are 1 March–30 November, 1 April–30 November, and 1 April–31 October, respectively. Most wildfires in the study area mainly occurred in shrub and grasslands. Most shrub and grass fires occurred in the period from June–September, and fires in mountain forests occurred mainly in the April–June and September–October periods.

The MNI index is a good indicator of fire danger for Central Asia. In the 2030s, the mean daily maximum temperature in the fire season for vegetation areas will increase significantly over the baseline, and the precipitation will increase by 7%–15%. The MNI will increase by 33%–68% for vegetation areas in the 2030s. The mean daily maximum temperature, precipitation and MNI of vegetation areas will increase significantly in the 2080s. The MNI will increase by 63%–146%, and the potential areas will increase by 3%–13% for each vegetation zone.

Author Contributions: X.Z. and X.T. conceived and designed the experiments; X.Z. wrote the original draft and edited the manuscript. X.T. wrote, reviewed and edited the manuscript; Y.Y. contributed on data collection and reviewed the manuscript. All authors have read and agreed to the published version of the manuscript.

Funding: This research was funded by (Strategic Priority Research Program of the Chinese Academy of Sciences) grant number (XDA20020202) and (Project of National Natural Science Foundation of China) grant number (31770695).

Conflicts of Interest: The authors declare no conflicts of interest.

References

1. Marlon, J.R.; Bartlein, P.J.; Carcaillet, C.; Gavin, D.G.; Harrison, S.P.; Higuera, P.E.; Prentice, I.C. Climate and human influences on global biomass burning over the past two millennia. *Nat. Geosci.* **2008**, *1*, 697–702. [CrossRef]
2. Girardin, M.P.; Portier, J.; Remy, C.C.; Ali, A.A.; Paillard, J.; Blarquez, O.; Bergeron, Y. Coherent signature of warming-induced extreme sub-continental boreal wildfire activity 4800 and 1100 years BP. *Environ. Res. Lett.* **2019**, *14*, 124042. [CrossRef]
3. Viatte, C.; Strong, K.; Patonwalsh, C.; Mendonca, J.; Oneill, N.T.; Drummond, J.R. Measurements of CO, HCN, and C2H6 Total Columns in Smoke Plumes Transported from the 2010 Russian Boreal Forest Fires to the Canadian High Arctic. *Atmos. Ocean* **2013**, *51*, 522–531. [CrossRef]
4. Arkhipov, V.; Moukanov, B.M.; Khaidarov, K.; Goldammer, J.G. Overview on forest fires in Kazakhstan. *Int. For. Fire News* **2000**, *22*, 40–48. Available online: http://hdl.handle.net/11858/00-001M-0000-0014-9566-B (accessed on 10 May 2020).
5. Keyser, A.R.; Westerling, A.L. Predicting increasing high severity area burned for three forested regions in the western United States using extreme value theory. *For. Ecol. Manag.* **2019**, *432*, 694–706. [CrossRef]
6. Tansey, K.; Grégoire, J.M.; Stroppiana, D.; Sousa, A.; Silva, J.M.; Pereira, J.M.; Peduzzi, P. Vegetation burning in the year 2000: Global burned area estimates from SPOT VEGETATION data. *J. Geophys. Res. Atmos.* **2004**, *109*, D14S03. [CrossRef]
7. Atkin, M. Inside Central Asia: A Political and Cultural History of Uzbekistan, Turkmenistan, Kazakhstan, Kyrgyzstan, Tajikistan, Turkey, and Iran by Dilip Hiro. *Int. J. Middle East Stud.* **2011**, *43*, 190–192. [CrossRef]
8. Kleine, M.; Colak, A.H.; Kirca, S.; Saghebtalebi, K.; Orozumbekov, A.; Lee, D.K. Rehabilitating degraded forest landscapes in West and Central Asia. *IUFRO World Ser.* **2009**, *20*, 5–26.
9. Liu, Y.; Stanturf, J.; Goodrick, S. Trends in global wildfire potential in a changing climate. *For. Ecol. Manag.* **2010**, *259*, 685–697. [CrossRef]
10. Flannigan, M.; Cantin, A.S.; De Groot, W.J.; Wotton, M.; Newbery, A.; Gowman, L.M. Global wildland fire season severity in the 21st century. *For. Ecol. Manag.* **2013**, *294*, 54–61. [CrossRef]
11. AghaKouchak, A.; Huning, L.S.; Chiang, F.; Sadegh, M.; Vahedifard, F.; Mazdiyasni, O.; Mallakpour, I. How do natural hazards cascade to cause disasters? *Nature* **2018**, *561*, 458–460. [CrossRef] [PubMed]
12. Liang, S.; Hurteau, M.D.; Westerling, A.L. Large-scale restoration increases carbon stability under projected climate and wildfire regimes. *Front. Ecol. Environ.* **2018**, *16*, 207–212. [CrossRef]
13. San-Miguel-Ayanz, J.; Durrant, T.; Boca, R.; Libertà, G.; Branco, A.; de Rigo, D.; Ferrari, D.; Maianti, P.; Artés Vivancos, T.; Costa, H.; et al. *Forest Fires in Europe, Middle East and North Africa 2017*; Publications Office of the European Union: Luxemburg, 2018; EUR 29318; ISBN 978-92-79-92831-4. [CrossRef]
14. Kovats, R.S.; Valentini, R.; Bouwer, L.M.; Georgopoulou, E.; Jacob, D.; Martin, E.; Rounsevell, M.; Soussana, J.F. Europe. In *Climate Change 2014: Impacts, Adaptation, and Vulnerability. Part B: Regional Aspects. Contribution of Working Group II to the Fifth Assessment Report of the Intergovernmental Panel on Climate Change*; Barros, V.R., Field, C.B., Dokken, D.J., Mastrandrea, M.D., Mach, K.J., Bilir, T.E., Chatterjee, M., Ebi, K.L., Estrada, Y.O., Genova, R.C., et al., Eds.; Cambridge University Press: Cambridge, UK, 2015.
15. Wotton, B.M.; Nock, C.A.; Flannigan, M.D. Forest fire occurrence and climate change in Canada. *Int. J. Wildland Fire* **2010**, *19*, 253–271. [CrossRef]
16. Torzhkov, I.O.; Kushnir, E.A.; Konstantinov, A.V.; Koroleva, T.; Efimov, S.V.; Shkolnik, I.M. Assessment of Future Climate Change Impacts on Forestry in Russia. *Russ. Meteorol. Hydrol.* **2019**, *44*, 180–186. [CrossRef]
17. Klein, I.; Gessner, U.; Kuenzer, C. Regional land cover mapping and change detection in Central Asia using MODIS time-series. *Appl. Geogr.* **2012**, *35*, 219–234. [CrossRef]

18. Goldammer, J.G.; Davidenko, E.P.; Kondrashov, L.G.; Ezhov, N.I. Recent trends of forest fires in Central Asia and opportunities for regional cooperation in forest fire management. In Proceedings of the Regional Forest Congress Forest Policy: Problems and Solutions, Bishkek, Kyrgyzstan, 25–27 November 2004.
19. Kazakhstan International Security Exhibition. 2012 Forest Fires in Kazakhstan up by 41%. Available online: https://www.aips.kz/en/home/9-press-center/news/137-forest-fires-in-kazakhstan-up-by-41 (accessed on 18 June 2020).
20. Cao, X.; Meng, Y.; Chen, J. Mapping grassland wildfire risk of the world. In *World Atlas of Natural Disaster Risk*; Springer: Berlin/Heidelberg, Germany, 2015; pp. 277–283.
21. Loboda, T.V.; Giglio, L.; Boschetti, L.; Justice, C.O. Regional fire monitoring and characterization using global NASA MODIS fire products in dry lands of Central Asia. *Front. Earth Sci.* **2012**, *6*, 196–205. [CrossRef]
22. Warneke, C.; Bahreini, R.; Brioude, J.; Brock, C.A.; De Gouw, J.A.; Fahey, D.W.; Veres, P.R. Biomass burning in Siberia and Kazakhstan as an important source for haze over the Alaskan Arctic in April 2008. *Geophys. Res. Lett.* **2009**, *36*, L02813. [CrossRef]
23. Babu, K.V.S.; Kabdulova, G.; Kabzhanova, G. Developing the Forest Fire Danger Index for the Country Kazakhstan by Using Geospatial Techniques. *J. Environ. Inf. Lett* **2019**, *1*, 48–59. [CrossRef]
24. Spivak, L.; Arkhipkin, O.; Sagatdinova, G. Development and prospects of the fire space monitoring system in Kazakhstan. *Front. Earth Sci.* **2012**, *6*, 276–282. [CrossRef]
25. Van Wagner, C.E.; Forest, P. *Development and Structure of the Canadian Forest Fire Weather Index System*; Forestry Technical Report; Canadian Forestry Service: Ottawa, ON, Canada, 1987; p. 35.
26. Bedia, J.; Herrera, S.; Gutiérrez, J.M.; Benali, A.; Brands, S.; Mota, B.; Moreno, J.M. Global patterns in the sensitivity of burned area to fire-weather: Implications for climate change. *Agric. For. Meteorol.* **2015**, *214*, 369–379. [CrossRef]
27. Nesterov, V.G. *Forest fire Potential and Methods of Its Determination*; Goslesbumizdat Publishing House: Moscow, Russia, 1949.
28. Zhdanko, V.A. Scientific basis of development of regional scales and their importance for forest fire management. In *Contemporary Problems of Forest Protection from Fire and Firefighting*; Melekhov, I.S., Ed.; Lesnaya Promyshlennost Publishing: Moscow, Russia, 1965.
29. Sherstyukov, B.G. *Index of Forest Fire. Yearbook of Weather, Climate and Ecology of Moscow*; Moscow State University Publishing: Moscow, Russia, 2002.
30. Ganatsas, P.; Antonis, M.; Marianthi, T. Development of an adapted empirical drought index to the Mediterranean conditions for use in forestry. *Agric. For. Meteorol.* **2011**, *151*, 241–250. [CrossRef]
31. Niu, R.; Zhai, P. Study on forest fire danger over Northern China during the recent 50 years. *Clim. Chang.* **2012**, *111*, 723–736. [CrossRef]
32. Karouni, A.; Daya, B.; Bahlak, S. A comparative study to find the most applicable fire weather index for Lebanon allowing to predict a forest fire. *J. Commun. Comput.* **2013**, *11*, 1403–1409. Available online: http://www.wanfangdata.com.cn/details/detail.do?_type=perio&id=David_20171208_2213 (accessed on 10 June 2020).
33. Groisman, P.Y.; Sherstyukov, B.G.; Razuvaev, V.N.; Knight, R.W.; Enloe, J.G.; Stroumentova, N.S.; Karl, T.R. Potential forest fire danger over Northern Eurasia: Changes during the 20th century. *Glob. Planet. Chang.* **2007**, *56*, 371–386. [CrossRef]
34. Mouillot, F.; Schultz, M.G.; Yue, C.; Cadule, P.; Tansey, k.; Ciais, P.; Chuvieco, E. Ten years of global burned area products from space borne remote sensing—A review: Analysis of user needs and recommendations for future developments. *Int. J. Appl. Earth Obs. Geoinf.* **2014**, *26*, 64–79. [CrossRef]
35. Hall, J.V.; Loboda, T.V.; Giglio, L.; Hall, J.V.; Loboda, T.V.; Giglio, L.; Mccarty, G.W. A MODIS-based burned area assessment for Russian croplands: Mapping requirements and challenges. *Remote Sens. Environ.* **2016**, *184*, 506–521. [CrossRef]
36. Zhu, C.; Kobayashi, H.; Kanaya, Y.; Zhu, C.; Kobayashi, H.; Kanaya, Y.; Saito, M. Size-dependent validation of MODIS MCD64A1 burned area over six vegetation types in boreal Eurasia: Large underestimation in croplands. *Sci. Rep.* **2017**, *7*, 1–9. [CrossRef]
37. Ruan, H.W.; Yu, J.J. Changes in land cover and evapotranspiration in the five CentralAsian countries from 1992 to 2015. *Acta Geogr. Sin.* **2019**, *74*, 1292–1304. [CrossRef]

38. Yang, G.; Teng, Y.; Shu, L.F.; Cai, H.Y.; Di, X.Y. Review of Forest and Grassland Fire Prevention Along "the Belt and Road". *World For. Res.* **2018**, *31*, 82–88. [CrossRef]
39. Global Forest Resources Assessment 2015. Available online: http://www.fao.org/3/a-au190e.pdf (accessed on 10 June 2020).